https://doi.org/10.5194/egusphere-2026-4227
Preprint. Discussion started: 19 August 2026

Beyond saturation zones: localized hydrobiogeochemical heterogeneity shapes microbial functional profiles across an arid critical zone

María J. Salinas-Bonillo[1,2], María J. López[1,4], Lucía Cabello-Alemán[2], Montserrat Escudero-Clares[1,2], Claudia Guillén[1], Ángel Fernández-Cortés[1,2], Juan Gisbert-Gallego[1,3], María R. Martínez-Gallardo[1,4], Javier Cabello[1,2]

[1] Department of Biology and Geology, University of Almería, Almería, 04120, Spain
[2]Andalusian Centre for Global Change (ENGLOBA), University of Almería, 04120 Almería, Spain
[3]Research Centre for Scientific Collections (CECOUAL), University of Almería, 04120 Almería, Spain
[4]Research Centre for Mediterranean Intensive Agrosystems and Agri-Food Biotechnology (CIAIMBITAL), University of Almería, Almería, 04120, Spain

Correspondence to: María J. Salinas-Bonillo (mjsalina@ual.es)

Abstract. Conceptual models of the Critical Zone (CZ) have been developed primarily in humid and temperate settings, where subsurface organization is often described as a function of continuous vertical gradients in hydrology, weathering, and biogeochemical development. The extent to which this vertical-gradient framework applies to arid CZs - where water limitation, episodic recharge, and spatially discontinuous resource distributions dominate - remains largely unexplored. Here, we evaluated whether microbial functional organization across an arid CZ follows broad saturated-unsaturated zonation or is instead shaped by localized hydrobiogeochemical heterogeneity. We combined community-level physiological profiles (CLPPs) with analyses of substrate organic matter (OM) quantity and quality (estimated from $\delta^{13}C$ signatures), substrate texture, and groundwater hydrochemistry from samples collected at multiple depths from eight boreholes spanning the unsaturated-saturated continuum of a groundwater-dependent ecosystem dominated by the facultative phreatophyte *Ziziphus lotus* (L.) Lam. in an arid Mediterranean setting. Microbial functional responses derived from carbon-source-use patterns were not primarily structured by saturated-unsaturated zonation per se. Instead, OM availability emerged as the dominant driver of both general microbial functional metrics and the utilization of several carbon-source groups, whereas OM quality exerted more selective effects on carbon-source-use patterns, altering the relative importance of different carbon-source groups under increasingly processed OM conditions. Substrate texture modulated these responses, with sandy fractions generally constraining microbial activity, although these effects were partially compensated by higher OM availability. Notably, groundwater-table position, groundwater hydrochemistry, proximity to *Z. lotus* individuals, and *Z. lotus* greenness did not emerge as significant drivers. In particular, the absence of relationships with either proximity to *Z. lotus* or its vegetation greenness indicates that the influence of this phreatophyte may be largely restricted to localized zones rather than extending across the broader subsurface matrix. These findings suggest that microbial functioning in arid CZs may be

https://doi.org/10.5194/egusphere-2026-4227
Preprint. Discussion started: 19 August 2026

organized around spatially discontinuous hydrobiogeochemical resource patches and localized habitat heterogeneity rather than around the vertically structured gradients that characterize many humid-climate CZ conceptual models.

Graphical Abstract

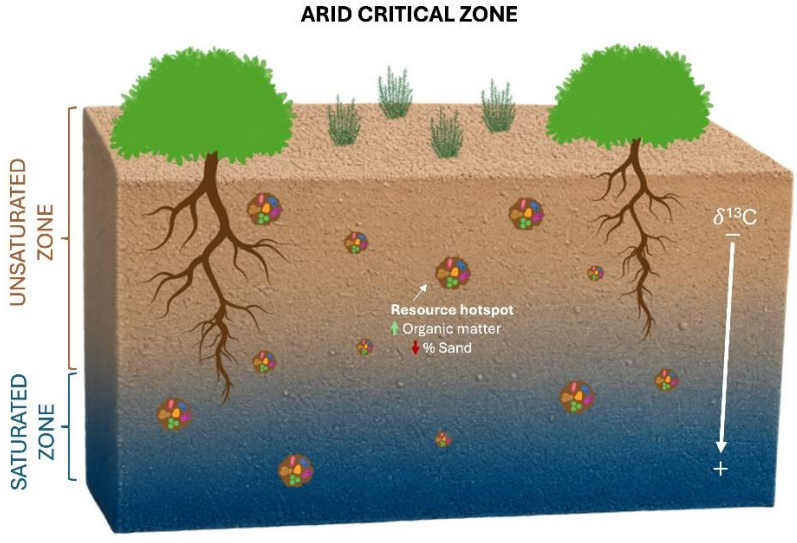

1 Introduction

The Critical Zone (CZ), defined as the near-surface layer extending from the vegetation canopy to the groundwater system, is one of the most intensively studied interfaces in Earth system science (National Research Council, 2001; Brantley et al., 2007; Chorover et al., 2007). Much of the conceptual architecture of CZ science, however, has been built on observations from humid and temperate systems, where subsurface organization is typically described as a function of continuous vertical gradients in weathering intensity, hydrological connectivity, and biogeochemical development (Brantley et al., 2007; Rempe and Dietrich, 2018). Within this framework, the transition between unsaturated (USZ) and saturated (SZ) zones is often treated as a key biogeochemical boundary, where shifts in water saturation, oxygen availability, solute transport, and redox conditions are commonly expected to generate vertical structure in microbial functioning and organic matter (OM) transformation (Akob and Küsel, 2011; Zhang and Furman, 2021). Whether this vertical-gradient framework applies beyond humid and temperate settings, particularly in arid CZs where the fundamental assumptions of continuous hydrological connectivity and gradual resource depletion with depth may not hold, remains largely untested.

Among the factors potentially regulating microbial functioning across the subsurface CZ continuum, OM quantity and quality, substrate texture, and hydrogeochemical gradients are likely to play major roles. OM quantity and quality are widely recognized as key regulators of microbial activity and C cycling within terrestrial and subsurface environments (Fierer et al.,

https://doi.org/10.5194/egusphere-2026-4227
Preprint. Discussion started: 19 August 2026

2003; Schimel et al., 2007; Lehmann and Kleber, 2015). Along CZ profiles, vertical changes in OM accumulation, accessibility, and biogeochemical transformation may substantially modify C-source use and microbial functioning (Lehmann and Kleber, 2015; Soldatova et al., 2024). In particular, stable C isotopic signatures ($\delta^{13}C$) provide integrative information on OM origin, turnover, and degree of microbial transformation, with isotopic enrichment generally associated with increasingly processed and older C pools (Ehleringer et al., 2000; Bowling et al., 2008). At the same time, substrate texture may regulate microbial functioning by influencing water retention, oxygen diffusion, pore connectivity, and the physical protection and stabilization of OM within aggregates and porous media (Six et al., 2002; Or et al., 2007). Some studies in CZs have further highlighted strong linkages between geochemical organization, OM transformation, and microbial community functioning, emphasizing the role of hydrobiogeochemical heterogeneity in structuring subsurface ecosystem processes (Brantley et al., 2007; Wu et al., 2023).

In arid CZs, localized hydrobiogeochemical heterogeneity may be as important as broad vertical gradients in regulating subsurface microbial functioning. Limited water availability, intense evapotranspiration, and episodic recharge events generate pronounced spatial and temporal variability in hydrological connectivity and biogeochemical functioning (Schwinning and Sala, 2004; Or et al., 2007). Consequently, resource distributions are often spatially discontinuous, leading to localized hydrobiogeochemical hotspots (Or et al., 2007; Bastida et al., 2021). In these systems, groundwater-dependent ecosystems (GDEs) may buffer vegetation against drought stress by maintaining access to groundwater resources, thereby partially decoupling ecosystem functioning from direct precipitation inputs (Eamus et al., 2015; Torres-García et al., 2022). Deep-rooted phreatophytic species establish extensive root systems capable of linking surface and groundwater compartments across the CZ profile (Torres-García et al., 2021b), potentially influencing C inputs, rhizosphere activity, and microbial functioning at depth. However, rhizosphere effects are often highly localized and spatially heterogeneous, particularly in drylands where vegetation cover is patchy and resource availability varies markedly over short spatial scales (Or et al., 2007; Philippot et al., 2013).

Although previous studies have separately explored hydrogeochemical organization within the CZ (Akob and Küsel, 2011; Wu et al., 2023) and the ecohydrological functioning of GDEs in drylands (Eamus et al., 2015; Torres-García et al., 2021a,b, 2022), integrated evaluations of how hydrobiogeochemical conditions and GDE-related gradients jointly regulate microbial functioning across arid saturated-unsaturated transitions remain scarce. This study evaluated microbial functioning across the saturated-unsaturated continuum of an arid CZ associated with a GDE dominated by the facultative phreatophyte *Ziziphus lotus* (Torres-García et al., 2021a). Specifically, we investigated how variation in OM quantity and quality, substrate texture, groundwater hydrochemistry, groundwater-table position, vegetation greenness, and proximity to *Z. lotus* individuals influence both general and C-source-specific microbial responses along the CZ profile. We hypothesized that: H1) contrary to conceptual models developed for humid CZs, microbial functional organization in arid systems does not follow saturated-unsaturated zonation but is instead governed by spatially discontinuous hydrobiogeochemical heterogeneity, with microscale resource distribution acting as the primary organizational principle; H2) OM availability exerts strong controls on microbial functioning, as the spatially restricted and heterogeneous distribution of organic resources is expected to be the primary

https://doi.org/10.5194/egusphere-2026-4227
Preprint. Discussion started: 19 August 2026

bottleneck for microbial processes under strong water limitation; and H3) Because *Z. lotus* functions as a deep-rooted phreatophyte linking surface and groundwater compartments, we expected vegetation-related gradients (proximity to *Z. lotus* individuals and vegetation greenness) to influence microbial functioning through localized rhizosphere inputs and enhanced resource availability, potentially generating hotspots of microbial activity within the broader CZ matrix.

2 Materials and methods

2.1 Study area

The study was conducted in the semiarid coastal plain of Cabo de Gata-Níjar Natural Park, Southeast of Spain (36.830606−2.293612), where the phreatophyte *Ziziphus lotus* (L.) Lam. (Rhamnaceae) is the keystone species of a groundwater-dependent ecosystem (GDE) (Guirado et al., 2018; Torres-García et al., 2021b) (Fig. 1). Geologically, the area corresponds to the foothills of the Sierra Alhamilla sedimentary basin (1000 m a.s.l.), located approximately 20 km north of the study site, and to overlying Quaternary marine deposits (Vallejos et al., 2018). The plain is located over a shallow aquifer connected to the western sector of the Hornillo-Cabo de Gata aquifer system (Vallejos et al., 2018). The climate is semiarid Mediterranean, characterized by hot, dry summers and mild winters. Mean annual temperature is approximately 18 °C, and annual precipitation averages 220 mm, occurring mainly during autumn and winter (Machado et al., 2011). Groundwater depth, measured from the ground surface to the water table, ranges from 2.2 to 25.2 m, with slight seasonal increases from spring to summer (based on long-term monitoring records collected from the study boreholes between 2019 and 2024). *Z. lotus* is a winter-deciduous shrub highly adapted to arid environments due to its extensive root system, which can reach depths of up to 60 m (Le Houérou, 2006), and its strong dependence on groundwater resources (Guirado et al., 2018), which allows it to thrive during the dry summer period (Torres-García et al., 2021b). The species typically forms hemispherical shrub patches ranging from 3 to 5 m in height and covering mean areas of 100 m² (Guirado et al., 2019), creating patchy vegetation islands interspersed with smaller shrubs and generating a characteristic heterogeneous spatial structure in arid landscapes (Tirado, 2009).

https://doi.org/10.5194/egusphere-2026-4227
Preprint. Discussion started: 19 August 2026

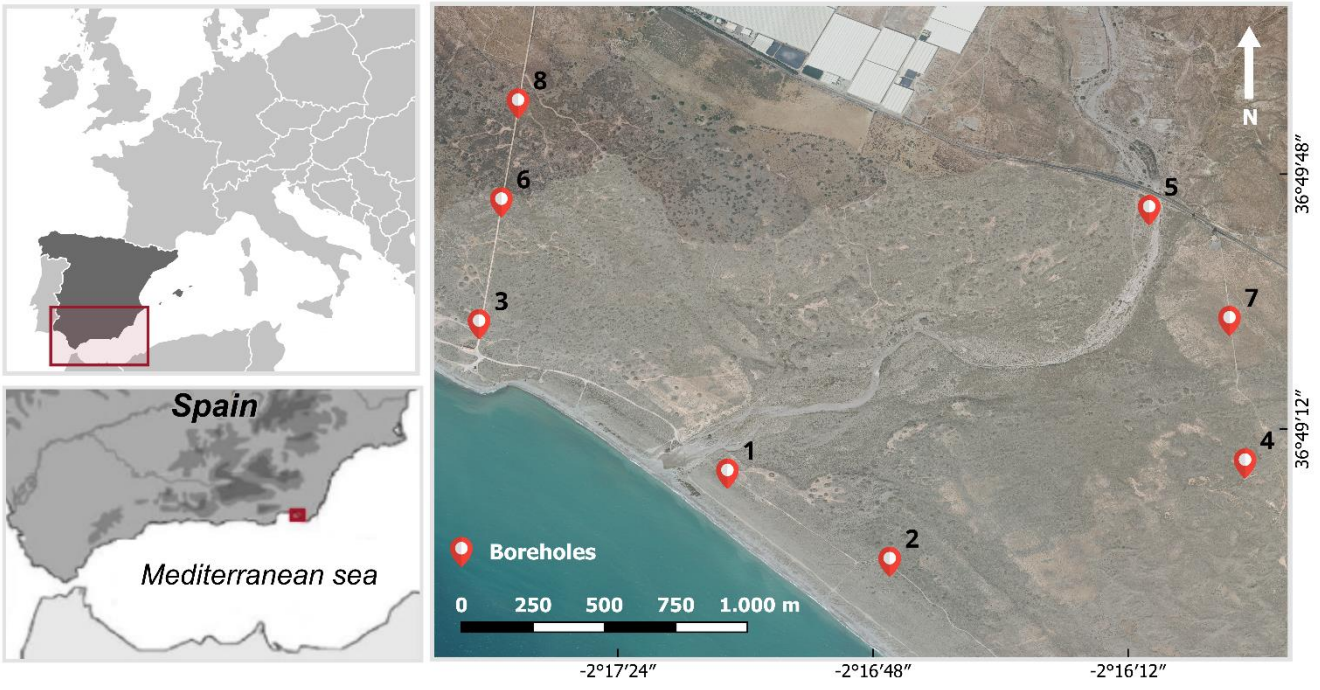

Figure 1. Location of the study area in the coastal plain of Cabo de Gata-Níjar Natural Park (southeastern Spain) and spatial distribution of the eight boreholes. Boreholes are numbered according to increasing depth to the groundwater table. Base orthophotograph from the Spanish National Plan for Aerial Orthophotography (PNOA).

2.2 Sampling

Substrate samples were collected between December 2018 and January 2019 from eight boreholes distributed throughout the study area using a rotary drilling system. Samples were retrieved at 5 m intervals to minimize vertical mixing and potential cross-contamination among successive depth sections. A total of 58 samples were obtained from at least four depths per borehole across a depth range of 1-40 m, reaching a depth of 40 m in some boreholes (nine samples) (Table S1). Samples were immediately stored in sealed bags, transported in a cool box, and preserved at -20 °C until analysis. In addition, 1 L substrate samples were taken for granulometric analysis.

Groundwater depth (DTGW) was monitored in the boreholes between 2019 and 2024 using HOBO® U20 water-level sensors that recorded hourly measurements. DTGW ranged from 2.2 m (borehole 1) to 25.2 m (borehole 8), with fluctuations between 0.4 and 1.2 m. To characterize groundwater physicochemistry, water samples were collected from each borehole during different months between 2019 and 2022: May, September, and November in 2019; June, July, and September in 2020; March, May, July, September, and November in 2021; and May, July, September, and November in 2022. Based on their hydrological position, substrate samples were classified into two zones: the unsaturated zone (USZ), comprising samples above the groundwater table, and the saturated zone (SZ), comprising samples below it. To allow comparisons

https://doi.org/10.5194/egusphere-2026-4227
Preprint. Discussion started: 19 August 2026

among boreholes with different DTGW, the sample depth was standardized relative to the local groundwater table depth. Relative depth to groundwater (RDTGW) was calculated as (WT - z) / WT, where z is the sample depth, and WT is the groundwater-table depth at each borehole. This transformation sets the groundwater table to zero, with positive values indicating samples above the water table (USZ) and negative values indicating samples below it (SZ). RDTGW values were grouped into depth intervals separately for the USZ and SZ. Because the range of RDTGW differed markedly between zones, interval widths were defined independently to preserve the groundwater table (RDTGW = 0) as the boundary between saturated and unsaturated compartments while maintaining representative vertical partitioning within each zone. Accordingly, three intervals of 0.320 relative-depth units were defined in the USZ, whereas five broader intervals of 2.211 relative-depth units were defined in the SZ. Because the objective was to represent relative hydrobiogeochemical compartments along the saturated-unsaturated continuum rather than equivalent absolute depth ranges, these intervals were used only for descriptive and non-parametric comparisons, whereas continuous RDTGW values were retained for subsequent statistical modelling.

2.3 Laboratory analysis

2.3.1 Substrate texture, OM, and $\delta^{13}C$ composition

Substrate samples were analysed using conventional particle-size separation methods appropriate for detrital sedimentary materials. Coarse fractions (gravels and sands > 0.075 mm) were separated by dry sieving, whereas the fine fraction (silt and clay fractions < 0.075 mm) was quantified using standard sedimentation-based particle size analyses following Das and Sobhan (2018). Across both hydrological zones and depth intervals, the substrate was predominantly coarse-grained, with gravel and sand dominating, and only minor contributions from fine materials (Fig. S1), characteristic of coarse-beach sedimentary environments. The resulting proportions of sand and fine material fractions (%Sand and %Fine) were subsequently used in the statistical analyses and Bayesian models as descriptors of substrate texture. Gravel content was excluded from the models because it showed strong collinearity with the sand fraction.

The OM content (%) of the samples was determined gravimetrically by loss-on-ignition. Three aliquots (1 g) of each sample were weighed into pre-weighed crucibles and dried at 105 °C to remove moisture. After drying, the samples were weighed, combusted in a muffle furnace at 550 °C for 3.5 h, and weighed again after cooling. OM content was calculated as the mass loss after combustion and expressed as a percentage of the dry sample weight. Substrate δ13C measurements were used as an indicator of OM quality. Isotopic analyses were performed at the Stable Isotope Laboratory of the University of Almería (Almería, Spain). Three aliquots (~100 mg) of each sample were weighed into tin capsules and pyrolyzed at 550 °C using a combustion module (CM) coupled to a cavity ringdown spectroscopy (CRDS) System (G2201-i Analyzer, Picarro). This temperature threshold ensures that a loss-on-ignition analysis (Sparkes et al., 2026) yields CO_2 evolved exclusively from the combustion of all OM, whereas the inorganic C fraction is combusted at higher temperatures (Wang et al., 2011). Powdered samples were loaded into the CM by an autosampler (Costech Analytical Technologies, Valencia, CA, US), and the released

https://doi.org/10.5194/egusphere-2026-4227
Preprint. Discussion started: 19 August 2026

CO_2 was transferred to a Picarro Liaison A0301 interface and finally input into CRDS for analysis. The system assembly uses ultra-high purity N_2 as the carrier gas and pure O_2 for combustion. The C isotope ratios were expressed in ‰ using δ notation relative to the Vienna Pee Dee Belemnite (VPDB) standard. The raw δ13C values were calibrated against four in-house references: $NaHCO_3$, sugarcane, acetanilide, and urea, covering a wide calibration range from -4.2 ‰ to -43.4 ‰. Three replicates for each working reference standard were included in each analysis batch, except for acetanilide and $NaHCO_3$, of which 6 replicates were used to check and correct any instrumental drift. These reference standards were initially calibrated against several international standards supplied by the United States Geological Survey (USGS)/Reston Stable Isotope Laboratory (l-Glutamic acid standards USGS-40 and USGS-41a; with δ13C V-PDB values of -26.389 ‰ and 34.626 ‰, respectively) and IAEA (IAEA-603 and NBS-18 calcites, with δ13C V-PDB values of +2.460 ‰ and -5.014 ‰, respectively). Based on analyses of these standards, precision ranged from 0.06 to 0.71 ‰ (n=27), and accuracy, as measured by δ13C error, ranged from -0.33 to 0.68 %.

2.3.2 Microbial functional profiling using Biolog EcoPlates™

Microbial metabolic profiles were assessed using Biolog EcoPlates™ in substrate samples collected at different depths. This CLPP approach provides a widely used measure of microbial functional diversity and C-source utilization patterns by quantifying the capacity of microbial communities to metabolize different C sources (Preston-Mafham et al., 2002). It allows the evaluation of microbial functional responses to environmental gradients and has been extensively applied to investigate the influence of physicochemical conditions on microbial metabolism in terrestrial and subsurface environments (Feigl et al., 2017; Németh et al., 2021). This technique evaluates the utilization of 31 C sources, grouped into six functional categories by C-source type: amines, amino acids, carbohydrates, carboxylic acids, phenolic compounds, and polymers (Table S2). As such, they provide information on the metabolically active heterotrophic fraction of the microbial community. Consequently, the measured responses should be interpreted as potential community-level physiological profiles rather than direct measurements of in situ microbial processes. For microbial suspension preparation, 2 g of the sample was weighed onto sterile filter paper and transferred into a test tube containing 18 mL of sterile saline solution (0.9% w/v NaCl), corresponding to a 10^{-1} dilution. Suspensions were vortexed for 2 min using an RSLAB-6PRO vortex mixer. Serial decimal dilutions were subsequently prepared in sterile saline solution up to 10-3 and used for microplate inoculation. A 150 µL volume of the final dilution was added to each well of the Biolog EcoPlate™ using a multichannel pipette. Each EcoPlate™ consists of 96 wells arranged as three identical sets of 32 wells (31 C-sources plus one water control well), providing three technical replicates for each sample. The inoculated microplates were incubated at 25 °C for 72 h. This incubation period was selected as a standardized endpoint to ensure comparability among samples while providing sufficient time for microbial growth and C-source utilization without excessive colour development. Optical density (OD) was measured at $\lambda = 590$ nm using an EON BioTek spectrophotometer (BioTek Instruments, Inc., Winooski, VT, USA) following Garland (1996). For each replicate, the OD of the water control well was subtracted from the OD of the corresponding C-source wells to obtain corrected absorbance values. Corrected absorbance values below zero were set to zero. From these measurements, we calculated five

https://doi.org/10.5194/egusphere-2026-4227
Preprint. Discussion started: 19 August 2026

functional parameters: (1) C-source richness (SR), calculated as the number of C sources with corrected OD values above 0.25, a commonly used threshold to distinguish positive C-source utilization from background signal in Biolog EcoPlate™ assays (Garland, 1996); (2) average well colour development (AWCD), used as an indicator of overall microbial metabolic activity; (3) average well colour development for each C-source group (SAWCD), representing metabolic activity within each C-source category; (4) Shannon diversity (H′), reflecting the diversity of C-source utilization; and (5) Shannon evenness (E), indicating the equitability of C-source use among functional groups (Feigl et al., 2017).

2.3.3 Groundwater physicochemical characterization

Groundwater physicochemical characterization was based on in situ measurements of water temperature, pH, electrical conductivity (EC), dissolved oxygen (DO), and redox potential (Eh) using a portable multiparametric probe (HACH® HQ-30d, Loveland, CO, USA). Major ions (Ca, Mg, Na, K, Cl, SO_4^{2-}, HCO_3^-, F^- and Br^-), nutrients (NO_3^-), and dissolved elements (Al, B, Bi, Fe, Li, Mn, Rb, Si, Sr and S) were analysed at the CEBAS-CSIC Ionomic Service using standard hydrochemical methods and inductively coupled plasma optical emission spectrometry (ICP-OES) for elemental determinations.

2.4 NDVI-based vegetation activity assessment

To assess vegetation greenness associated with both *Z. lotus* and the surrounding arid shrubland matrix, we calculated the seasonal dynamics of the normalized difference vegetation index (NDVI; Rouse et al., 1974). NDVI derived from satellite imagery is widely used as a proxy for vegetation greenness and net primary productivity (Paruelo et al., 1997; Tian et al., 2017) and is calculated as:

$$\mathrm{NDVI} = \frac{(\mathrm{RNIR} - \mathrm{RRED})}{(\mathrm{RNIR} + \mathrm{RRED})}, \quad (1)$$

where RNIR is the reflectance of the near-infrared band, and RRED is the reflectance of the red band. We selected harmonized Sentinel-2 Level 2A surface reflectance images with a spatial resolution of 10 m $pixel^{-1}$ and a temporal resolution of five days. To ensure data quality, images were processed in Google Earth Engine, excluding pixels with a cloud or shadow probability greater than 10%. For *Z. lotus*, monthly NDVI values were calculated from cloud- and shadow-free pixels containing more than 75% *Z. lotus* cover and located within 5-100 m of each borehole. Depending on image availability after filtering, between 3 and 18 pixels per borehole were retained for the monthly calculations. NDVI values were averaged for the period from April to June during 2018–2024, corresponding to the peak foliar development period of this species (Torres-García et al., 2022). For the surrounding shrubland matrix, NDVI values were calculated from the 49 pixels surrounding each borehole location, after excluding cloud- and shadow-affected pixels. Monthly NDVI values for the shrubland matrix were therefore based on 42-44 pixels per borehole and averaged over February to April during 2018-2024,

https://doi.org/10.5194/egusphere-2026-4227
Preprint. Discussion started: 19 August 2026

corresponding to the peak greenness of this vegetation type. Although some of these pixels may have included *Z. lotus* individuals, the species is mostly leafless during this period.

2.5 Statistical analysis

All statistical analyses and graphical representations were performed in R (version 4.5.2; R Core Team). Differences in substrate OM content, $\delta^{13}C$, %Sand and %Fine, and microbial activity between the USZ and SZ were assessed with non-parametric Wilcoxon rank-sum tests (wilcox.test function, 'stats' package). Differences among relative-depth intervals were evaluated using Kruskal-Wallis tests followed by Dunn's post hoc multiple-comparison tests with adjusted p-values (kruskal.test function, 'stats' package; dunnTest function, 'FSA' package). Graphical representations of data across relative-depth intervals were created in the 'ggplot2' package using violin plots with embedded boxplots, allowing simultaneous visualization of data density, median, interquartile range, and mean values.

To characterize the dominant hydrochemical gradients across the study area, a principal component analysis (PCA) was performed using the mean values of the groundwater physicochemical variables measured in each borehole during the monitoring period (PCA function, 'FactoMineR' package). The dataset included water temperature, pH, electrical conductivity, dissolved oxygen, redox potential, major ions, nitrate, and dissolved elements. Prior to analysis, variables were standardized to zero mean and unit variance to account for differences in measurement scales and units. Because PCA is specifically designed to summarize covariance structures among interrelated variables, the full hydrochemical dataset was retained. The first two PCA axes (PCA1 and PCA2) (Fig. S4) were subsequently retained as synthetic descriptors of hydrogeochemical variability in the Bayesian models.

Bayesian mixed-effects models were fitted to evaluate the environmental drivers of CLPP-derived microbial functional responses across the CZ profile. Separate models were constructed for each of the global and C-source-specific microbial activity metrics using the 'brms' package. Models included OM content, $\delta^{13}C$, relative depth to groundwater (RDTGW), %Sand, %Fine, groundwater hydrochemistry descriptors (PCA1 and PCA2), NDVI associated with *Z. lotus* and total ecosystem vegetation, and the minimum distance from each borehole to the nearest *Z. lotus* individual as fixed effects. Prior to modelling, variables were transformed when required according to their distributional properties and data structure. OM content, NDVI metrics, and minimum distance to the nearest *Z. lotus* individual were log-transformed, and C-source richness was square-root transformed. Because substrate texture fractions (%sand, %fine material, and %gravel) represent compositional data constrained to a constant sum, they were transformed using a centred log-ratio (CLR) transformation. C-source utilization groups were Hellinger-transformed to reduce the dominance of highly utilized C-source groups while retaining information from less frequently utilized groups (Legendre and Gallagher, 2001). Subsequently, all continuous response variables and predictors included in the models were standardized (mean = 0, SD = 1) to facilitate model convergence and comparison of effect sizes among predictors. Ecologically meaningful interactions among predictors were explored to evaluate whether the effects of OM availability on microbial functioning depended on C quality, substrate texture, hydrogeochemical variability, or hydrological position along the CZ profile. Borehole identity was incorporated as a

https://doi.org/10.5194/egusphere-2026-4227
Preprint. Discussion started: 19 August 2026

random intercept to account for spatial dependence among samples collected within the same profile. Models were fitted under a Gaussian error distribution with weakly informative priors and four Markov chain Monte Carlo (MCMC) chains. Model convergence was assessed through visual inspection of trace plots and R-hat values < 1.01. Model comparison was performed using leave-one-out cross-validation (LOO-CV) implemented in the 'loo' package, retaining the most parsimonious model when predictive performance was similar among competing alternatives. For each predictor, we report the posterior mean regression coefficient (β), its 95% credible interval (CI), and the posterior probability associated with the direction of the effect (P (β > 0)). Positive and negative β values indicate positive and negative associations, respectively. Model interpretation focused on predictors showing strong directional posterior support, defined as P (β > 0) ≥ 0.95 or P (β > 0) ≤ 0.05.

3 Results

3.1 Factor variation along the CZ profile

Substrate OM content (%) increased towards the SZ, ranging from 0.31 to 8.00% (mean ± SD = 1.74 ± 1.30). OM values were significantly higher in the SZ (0.31-8.00%, 2.01 ± 0.48) than in the USZ (0.31-6.91%, 1.42 ± 0.96) (W = 4,647, p = 0.01) (Fig. S2). Along the relative-depth intervals, differences were primarily associated with higher OM values in the shallowest SZ interval [-2.211, 0] compared to the USZ interval [0.320, 0.640] (χ^2 = 24.96, p < 0.001) (Fig. S3). Substrate $\delta^{13}C$ signatures exhibited a pronounced vertical gradient across the CZ profile. Values ranged from -24.11 to -5.62‰ (mean ± SD = -13.75 ± 3.81), with significantly higher values in the SZ (-19.23 to -5.62‰, -11.96 ± 2.79) than in the USZ (-24.10 to -10.71‰, -15.89 ± 3.78) (W = 4,299, p < 0.001) (Fig. S2). Consistently, most SZ intervals showed significantly higher $\delta^{13}C$ values than USZ intervals, indicating progressively enriched isotopic signatures with depth (χ^2 = 52.64, p < 0.001; Fig. S3). Substrate fine material percentage (%Fine) ranged from 0.00 to 40.00% (mean ± SD = 5.19 ± 8.05). No significant differences were detected between the USZ (0.0-25.00%, 3.77 ± 5.05) and the SZ (1.00-40.00%, 6.34 ± 9.72) (W = 4,266, p = 0.10) (Fig. S2). Although %Fine showed a significant overall effect across relative-depth intervals (χ^2 = 18.53, p = 0.01), no significant pairwise differences were detected after Dunn's post hoc comparisons (Fig. S3). Substrate sand percentage (%Sand) ranged from 10.00 to 91.00% (58.07 ± 22.97). As for %Fine, no significant differences were observed between the USZ (10.00-89.00%, 55.00 ± 25.82) and the SZ (32.00-91.00%, 60.56 ± 20.16) (W = 4,072, p = 0.32) (Fig. S2). Across relative-depth intervals, %Sand showed significant differences within the SZ, with higher values in the shallowest interval [-2.211, 0] compared to the deepest interval [-11.054, -8.844] (χ^2 = 27.88, p < 0.001) (Fig. S3).

https://doi.org/10.5194/egusphere-2026-4227
Preprint. Discussion started: 19 August 2026

3.2 Microbial activity profiles

3.2.1 General microbial activity along the CZ profile

AWCD ranged from 0.00 to 0.71 (mean ± SD = 0.22 ± 0.10), and did not differ between the USZ (0.03-0.71, 0.23 ± 0.14) and the SZ (0.00-0.38, 0.21 ± 0.08) (W = 3,693, p = 0.88) (Fig. 2). No significant differences were detected among relative-depth intervals either (χ^2 = 11.24, p = 0.13) (Fig. 3). The Shannon diversity index (H′) varied from 0.00 to 1.74 (mean ± SD = 0.64 ± 0.46) and showed no significant differences between the USZ (0.00-1.74, 0.67 ± 0.58) and the SZ (0.00-1.38, 0.61 ± 0.33) (W = 3,611, p = 0.69) (Fig 2). Although the Kruskal-Wallis test indicated significant overall differences among relative-depth intervals (χ^2 = 16.52, p = 0.02), no significant pairwise differences were detected after Dunn's post hoc comparisons (Fig. 3). C-source richness (SR) ranged from 0 to 6 (mean ± SD = 2.11 ± 1.17) and was also comparable between the USZ (0-6, 2.33 ± 1.53) and the SZ (0-4, 1.93 ± 0.71) (W = 3,405, p = 0.27) (Fig. 2). As observed for H′, the Kruskal-Wallis test revealed significant overall differences among relative-depth intervals (χ^2 = 17.03, p = 0.02), although no significant pairwise differences were detected after Dunn's post hoc comparisons (Fig. 3). In contrast, Shannon evenness (E) showed clear differences across the CZ profile ranging from 0.00 to 1.00 (0.71 ± 0.43) and was significantly lower in the USZ (0.00-1.00, 0.62 ± 0.47) than in the SZ (0.00-1.00, 0.79 ± 0.38) (W = 5,006, p < 0.001) (Fig. 2). Across relative-depth intervals, E values remained relatively high throughout most of the profile, with no significant differences among USZ intervals (Fig. 3). Within the SZ, the shallowest interval near the groundwater transition ([-2.211, 0]) exhibited high E values (0.82 ± 0.36), differing significantly from the USZ intervals (χ^2 = 28.50, p < 0.001). A similar pattern was observed in the deeper SZ interval [-4.422, -2.211] (0.99 ± 0.01). In contrast, E dropped sharply in the interval [-8.844, -6.633] (0.00 ± 0.00), before recovering at greater depths in the interval [-11.054, -8.844] (0.64 ± 0.50), where no significant differences relative to the remaining USZ and SZ intervals were detected.

https://doi.org/10.5194/egusphere-2026-4227
Preprint. Discussion started: 19 August 2026

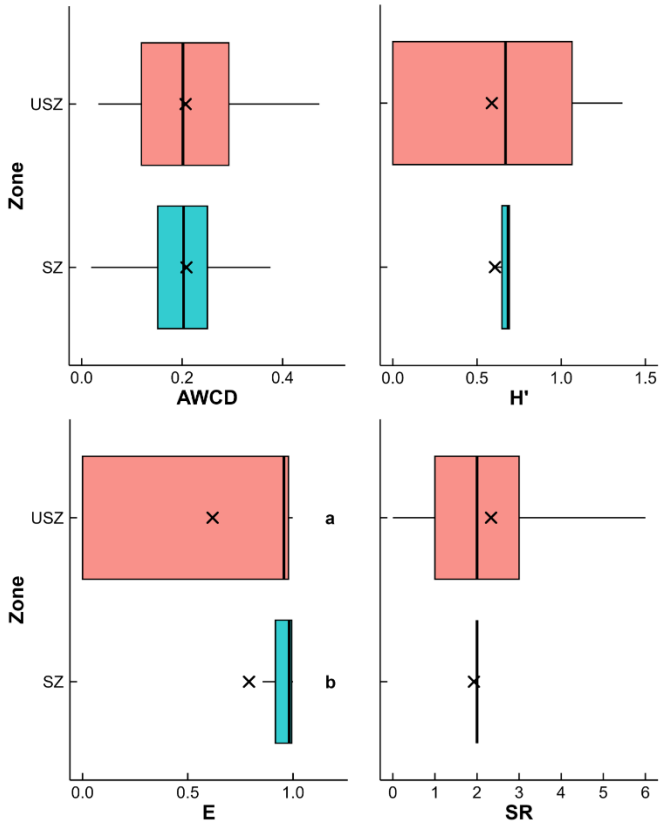

Figure 2. Box-and-whisker plots of four general microbial functional metrics in the unsaturated (USZ) and saturated (SZ) zones: average well colour development (AWCD), Shannon diversity (H′), Shannon evenness (E), and C-source richness (SR). Boxes represent the interquartile range (IQR), with the median shown by the central line, the mean marked by a cross, and whiskers extending to 1.5 × IQR. Different letters, where present, denote significant differences between hydrological zones according to Wilcoxon rank-sum tests ($p < 0.05$).

https://doi.org/10.5194/egusphere-2026-4227
Preprint. Discussion started: 19 August 2026

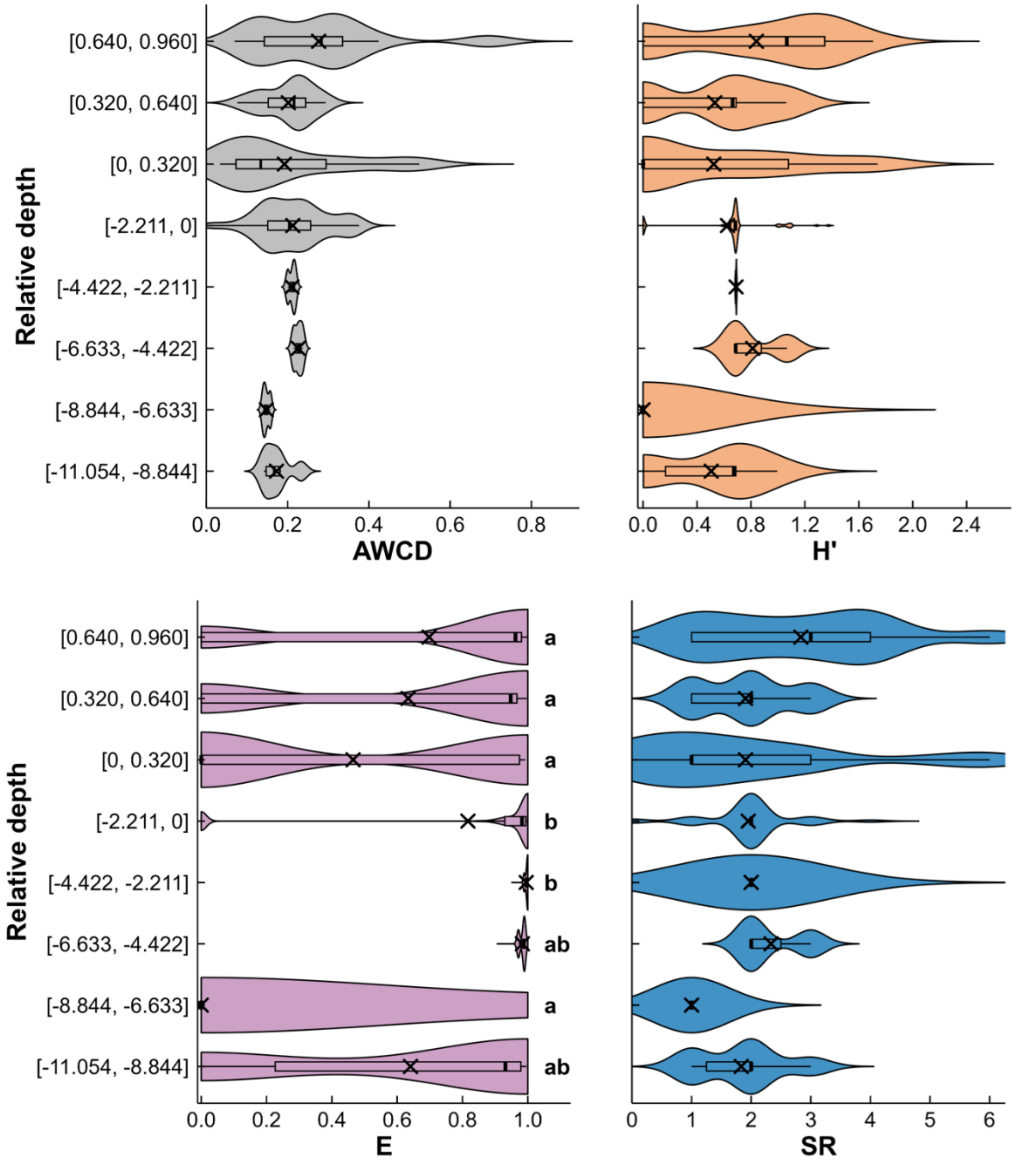

320

Figure 3. Violin plots showing the distribution of four general microbial functional metrics across depth intervals. Violin widths reflect the kernel density distribution of the data. Overlaid boxplots represent the interquartile range (IQR), with the median shown by the central line, the mean marked by a cross, and whiskers extending to 1.5 × IQR. Different letters, where present, denote significant differences among depth intervals according to Kruskal-Wallis tests followed by Dunn's post hoc tests ($p < 0.05$). AWCD, average well colour development; H′, Shannon diversity; E, Shannon evenness; SR, C-source richness.

325

https://doi.org/10.5194/egusphere-2026-4227
Preprint. Discussion started: 19 August 2026

3.2.2 Microbial activity by C-source type along the CZ profile

C-source-group utilization patterns varied among groups, although significant differences between the USZ and SZ were only detected for amines, phenolic compounds, and polymers (Fig. 4). Amine C-source utilization ranged from 0.00 to 0.59 (mean ± SD = 0.05 ± 0.11), with significantly higher values in the USZ (0.00-0.59, 0.09 ± 0.16) than in the SZ (0.00-0.12, 0.02 ± 0.02) (W = 3,070, p = 0.04) (Fig. 4). Across relative-depth intervals, the Kruskal-Wallis test indicated significant overall differences among groups (χ^2 = 16.92, p = 0.02), although Dunn's post hoc test did not detect significant pairwise differences (Fig. 5). Amino acid C-source utilization showed similar values in the USZ and SZ, ranging from 0.00 to 0.69 (mean ± SD = 0.17 ± 0.12). Values were slightly higher in the USZ (0.00-0.69, 0.19 ± 0.16) than in the SZ (0.00-0.40, 0.14 ± 0.07), although these differences were not significant (W = 3,619, p = 0.07) (Fig. 4). Likewise, no significant differences were detected among relative-depth intervals (χ^2 = 9.75, p = 0.20) (Fig. 5). Carbohydrate C-source utilization showed similar values in the USZ and SZ, ranging from 0.00 to 1.42 (mean ± SD = 0.19 ± 0.23). Values were higher in the USZ (0.00-1.42, 0.25 ± 0.31) than in the SZ (0.00-0.66, 0.13 ± 0.11), although these differences were not significant (W = 3,192, p = 0.09) (Fig. 4). Across relative-depth intervals, significant variation was detected (χ^2 = 15.93, p = 0.03), with carbohydrate utilization being significantly higher in the shallowest USZ interval [0.640, 0.960] (0.34 ± 0.39) than in the interval immediately adjacent to the groundwater transition [0, 0.320] (0.18 ± 0.23) (Fig. 5).

Carboxylic acid C-source utilization showed similar values in the USZ and SZ, ranging from 0.00 to 0.87 (mean ± SD = 0.38 ± 0.19). Values were slightly lower in the USZ (0.00-0.87, 0.34 ± 0.22) than in the SZ (0.00-0.75, 0.40 ± 0.16), although these differences were not significant (W = 4,377, p = 0.06) (Fig. 4). Although the Kruskal-Wallis test indicated significant overall differences among relative-depth intervals (χ^2 = 16.38, p = 0.02), Dunn's post hoc comparisons did not detect significant pairwise differences (Fig. 5). Phenolic C-source utilization was significantly higher in the USZ than in the SZ, ranging from 0.00 to 0.34 (mean ± SD = 0.03 ± 0.07). Values averaged 0.05 ± 0.10 in the USZ (0.00-0.34) and 0.01 ± 0.02 in the SZ (0.00-0.11) (W = 3,071, p = 0.02) (Fig.4). In contrast, no significant differences were detected among relative-depth intervals (χ^2 = 11.43, p = 0.12) (Fig. 5). Polymer C-source utilization ranged from 0.01 to 1.05 (mean ± SD = 0.51 ± 0.20), with significantly lower values in the USZ (0.03-1.00, 0.47 ± 0.19) than in the SZ (0.01-1.05, 0.54 ± 0.20) (W = 4,472, p = 0.03) (Fig. 4). Across relative-depth intervals, significant pairwise differences were detected between the USZ interval closest to the groundwater transition [0, 0.320] (0.34 ± 0.19) and the adjacent intervals immediately above [0.320, 0.640] (0.55 ± 0.14) and below the groundwater table [-2.211, 0] (0.55 ± 0.21) (χ^2 = 18.40, p = 0.01) (Fig. 5).

https://doi.org/10.5194/egusphere-2026-4227
Preprint. Discussion started: 19 August 2026

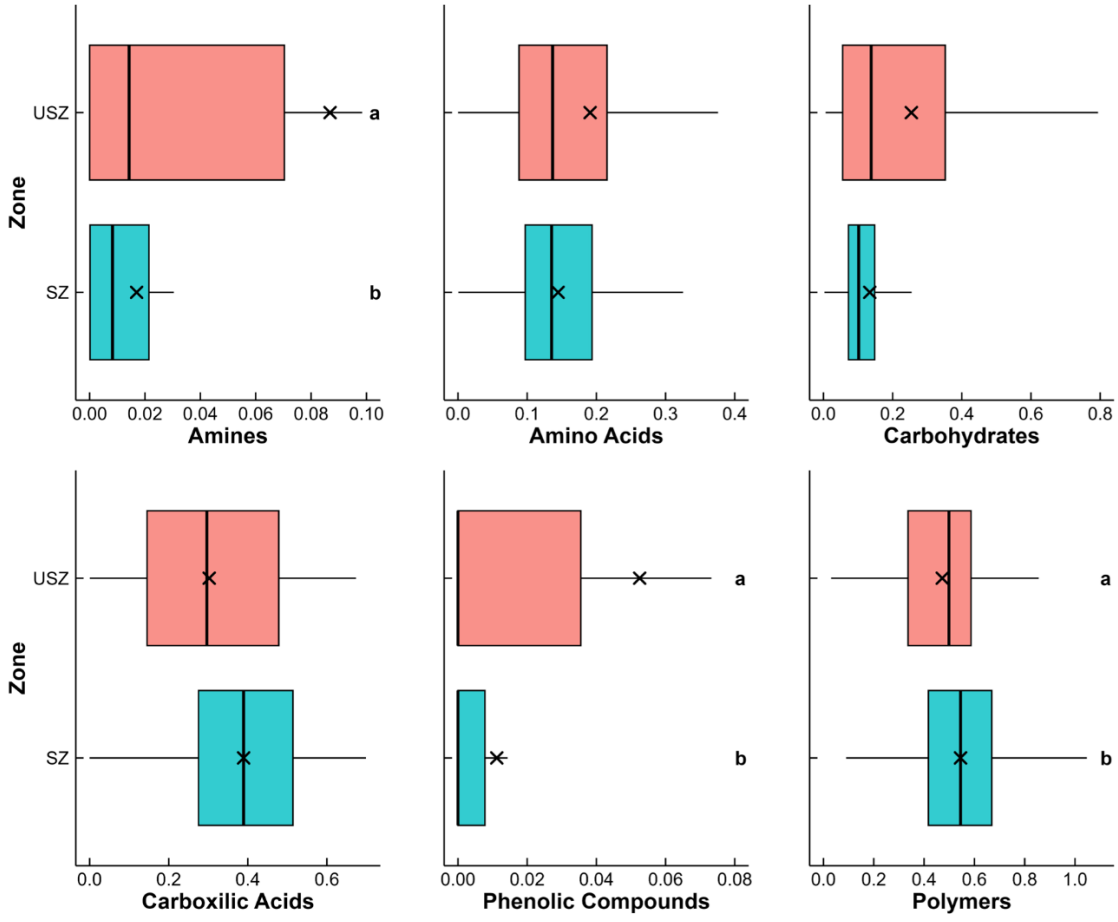

Figure 4. Box-and-whisker plots of microbial utilization of different carbon-source groups in the unsaturated (USZ) and saturated (SZ) zones. Boxes represent the interquartile range (IQR), with the median shown by the central line, the mean marked by a cross, and whiskers extending to 1.5 × IQR. Different letters, where present, denote significant differences between hydrological zones according to Wilcoxon rank-sum tests ($p < 0.05$).

https://doi.org/10.5194/egusphere-2026-4227
Preprint. Discussion started: 19 August 2026

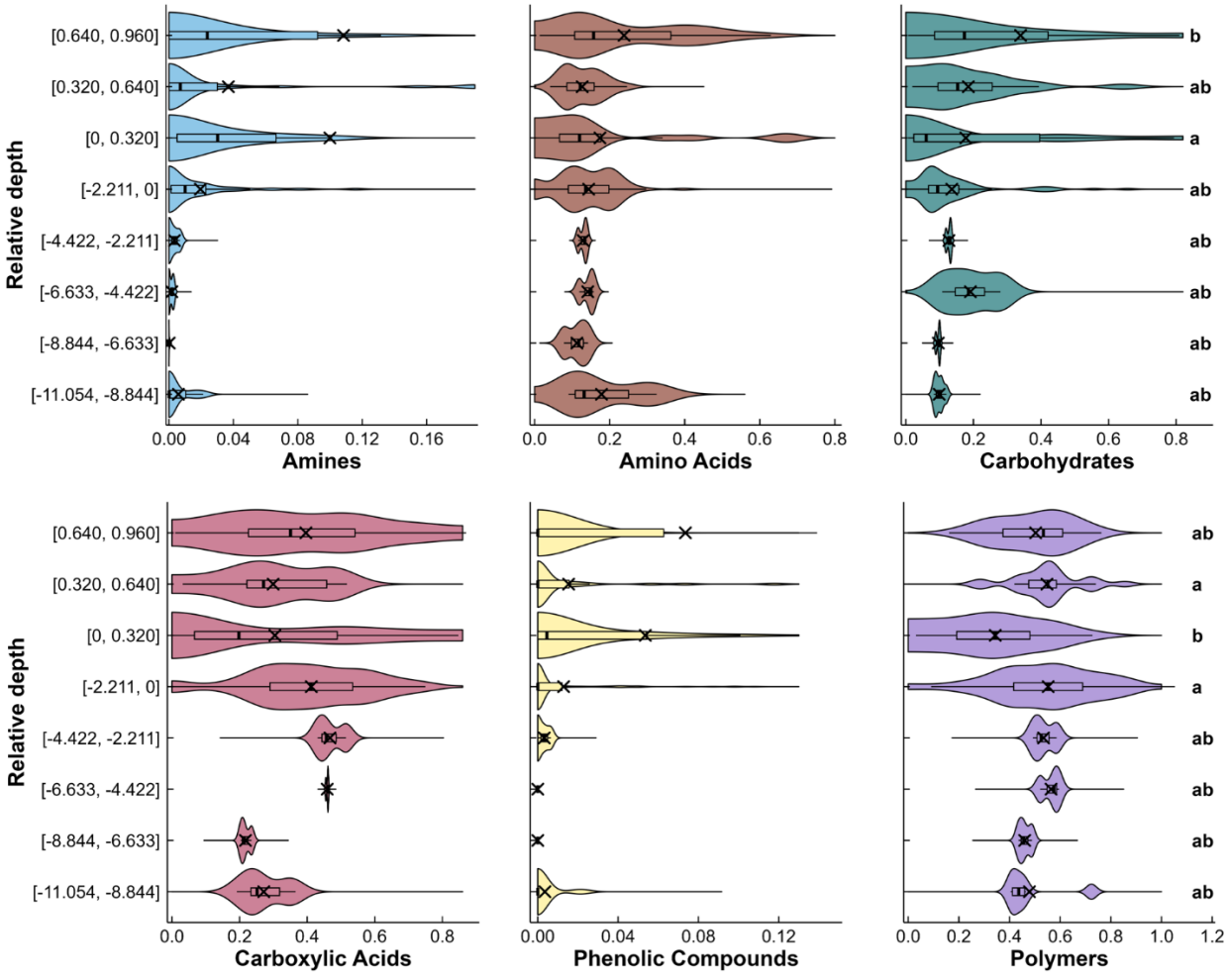

Figure 5. Violin plots showing the distribution of microbial utilization of different carbon-source groups across depth intervals. Violin widths reflect the kernel density distribution of the data. Overlaid boxplots represent the interquartile range (IQR), with the median shown by the central line, the mean marked by a cross, and whiskers extending to 1.5 × IQR. Different letters, where present, denote significant differences among depth intervals according to Kruskal-Wallis tests followed by Dunn's post hoc tests ($p < 0.05$).

3.3 Environmental drivers of microbial functioning across the CZ profile

3.3.1 Environmental drivers of general microbial functioning

OM content emerged as the dominant environmental driver of general microbial functioning, while substrate texture and OM quality modulated microbial responses (Table 1). AWCD was primarily associated with substrate OM content and fine

https://doi.org/10.5194/egusphere-2026-4227
Preprint. Discussion started: 19 August 2026

material content (%Fine), both exhibiting strong positive effects (β = 0.39, 95% CI: 0.22 to 0.55, P (β > 0) > 0.99; and β = 0.20, 95% CI: 0.02 to 0.38, P (β > 0) = 0.99, respectively) (Table 1). In contrast, substrate $\delta^{13}C$ values and sand content (%Sand) showed negative effects on AWCD (β = -0.20, 95% CI: -0.40 to -0.00, P (β > 0) = 0.02; and β = -0.20, 95% CI: -0.37 to -0.03, P (β > 0) = 0.01, respectively). A negative interaction between $\delta^{13}C$ values and OM content was also detected (β = -0.27, 95% CI: -0.43 to -0.10, P (β > 0) < 0.01), indicating that the positive effect of OM content on microbial metabolic activity weakened under increasingly ^{13}C-enriched conditions. Functional diversity (H′) was positively associated with OM content (β = 0.39, 95% CI: 0.22 to 0.55, P (β > 0) > 0.99), whereas %Sand showed a strong negative association (β = -0.34, 95% CI: -0.51 to -0.17, P (β > 0) < 0.01). A similar negative interaction between $\delta^{13}C$ values and OM content was detected (β = -0.27, 95% CI: -0.43 to -0.10, P (β > 0) < 0.01), consistent with the pattern observed for AWCD. Evenness (E) was positively associated with OM content and %Fine (β = 0.34, 95% CI: 0.18 to 0.51, P (β > 0) > 0.99; and β = 0.19, 95% CI: 0.01 to 0.37, P (β > 0) = 0.98, respectively), whereas %Sand showed a negative association (β = -0.31, 95% CI: -0.48 to -0.15, P (β > 0) < 0.01). C-source richness (SR) was strongly and positively associated with OM content (β = 0.50, 95% CI: 0.32 to 0.68, P (β > 0) > 0.99), whereas %Sand showed a marked negative association (β = -0.44, 95% CI: -0.63 to -0.26, P (β > 0) < 0.01). The same $\delta^{13}C$ × OM interaction was observed for SR (β = -0.25, 95% CI: -0.42 to -0.09, P (β > 0) < 0.01), together with a positive interaction between %Sand and OM content (β = 0.23, 95% CI: 0.07 to 0.39, P (β > 0) > 0.99).

https://doi.org/10.5194/egusphere-2026-4227
Preprint. Discussion started: 19 August 2026

Table 1. Summary of the most parsimonious Bayesian models explaining variation in four general microbial functional metrics: average well colour development (AWCD), Shannon diversity (H′), Shannon evenness (E), and carbon-source richness (SR). RDTGW, relative depth to the groundwater table; OM, organic matter content of geological substrate (%); $\delta^{13}C$, stable carbon isotope composition of geological substrate; %Fine, fine fraction of geological substrate (%); %Sand, sand fraction of geological substrate (%); PCA1 and PCA2, scores of the first and second principal component axes, respectively, derived from groundwater physicochemical variables; Min_Dist_Z, minimum distance (m) from each borehole to the nearest *Ziziphus lotus* individual. Bold values indicate parameter estimates with strong posterior support, defined as 95% credible intervals that do not overlap zero.

Microbiological response		**AWCD**	**H'**	**E**	**C-source richness**
Best model		δ13C x OM + RDTGW + %Fine + %Sand + PCA1+ PCA2 + Min_Dist_Z			δ13C x OM + %Sand x OM + RDTGW + %Fine + PCA1 + PCA2 + Min_Dist_Z
SD (Bore random effect)		0.40	0.39	0.35	0.29
Sigma		0.85	0.86	0.86	0.87
Total R^2		0.36	0.31	0.30	0.31
(95% CI)		(0.25, 0.45)	(0.20, 0.40)	(0.20, 0.40)	(0.22, 0.41)
Intercept	Mean	0.04	0.05	0.05	-0.04
	95% CI	-0.31, 0.39	-0.30, 0.39	-0.26, 0.39	-0.34, 0.27
	P (β > 0)	0.61	0.63	0.66	0.36
RDTGW	Mean	0.04	0.08	0.03	0.07
	95% CI	-0.15, 0.24	-0.12, 0.28	-0.16, 0.23	-0.13, 0.26
	P (β > 0)	0.67	0.79	0.63	0.75
OM	Mean	**0.39**	**0.39**	**0.34**	**0.50**
	95% CI	**0.22, 0.55**	**0.22, 0.55**	**0.18, 0.51**	**0.32, 0.68**
	P (β > 0)	**> 0.99**	**> 0.99**	**> 0.99**	**> 0.99**
δ13C	Mean	**-0.20**	-0.03	0.17	0.01
	95% CI	**-0.40, -0.00**	-0.22, 0.17	-0.03, 0.36	-0.19, 0.21
	P (β > 0)	**0.02**	0.39	0.95	0.56
%Fine	Mean	**0.20**	0.15	**0.19**	-0.08
	95% CI	**0.02, 0.38**	-0.03, 0.33	**0.01, 0.37**	-0.28, 0.13
	P (β > 0)	**0.99**	0.95	**0.98**	0.21
%Sand	Mean	**-0.20**	**-0.34**	**-0.31**	**-0.44**
	95% CI	**-0.37, -0.03**	**-0.51, -0.17**	**-0.48, -0.15**	**-0.63, -0.26**
	P (β > 0)	**0.01**	**< 0.01**	**< 0.01**	**< 0.01**
PCA1	Mean	0.28	0.16	0.10	0.21
	95% CI	-0.09, 0.60	-0.19, 0.48	-0.23, 0.41	-0.12, 0.48
	P (β > 0)	0.94	0.86	0.78	0.93
PCA2	Mean	-0.21	-0.03	0.08	-0.03
	95% CI	-0.62, 0.24	-0.44, 0.39	-0.37, 0.47	-0.41, 0.35
	P (β > 0)	0.85	0.44	0.67	0.43
Min_Dist_Z	Mean	-0.20	-0.00	0.17	-0.01
	95% CI	-0.67, 0.30	-0.46, 0.46	-0.29, 0.59	-0.40, 0.41
	P (β > 0)	0.84	0.49	0.81	0.48
δ13C x OM	Mean	**-0.27**	**-0.27**	-0.12	**-0.25**

https://doi.org/10.5194/egusphere-2026-4227
Preprint. Discussion started: 19 August 2026

	95% CI	**-0.43, -0.10**	**-0.43, -0.10**	-0.29, 0.04	**-0.42, -0.09**
	P (β > 0)	**< 0.01**	**< 0.01**	0.07	**< 0.01**
	Mean	--	--	--	**0.23**
%Sand x OM	95% CI	--	--	--	**0.07, 0.39**
	P (β > 0)	--	--	--	**> 0.99**

3.3.2 Environmental drivers of C-source utilization

OM availability consistently influenced the utilization of several C-source groups, whereas OM quality and substrate texture exerted more selective effects on specific metabolic pathways (Table 2). Amine and amino-acid utilization did not receive strong posterior support for any of the environmental predictors included in the models (Table 2). Carbohydrate utilization was positively associated with OM content (β = 0.20, 95% CI: 0.02 to 0.38, P (β > 0) = 0.99) and negatively associated with %Sand (β = -0.18, 95% CI: -0.36 to 0.00, P (β > 0) = 0.03). A negative interaction between $\delta^{13}C$ values and OM content was also detected (β = -0.20, 95% CI: -0.37 to -0.02, P (β > 0) = 0.01). Carboxylic acid utilization increased with both OM content and $\delta^{13}C$ values (β = 0.41, 95% CI: 0.22 to 0.60, P (β > 0) > 0.99; and β = 0.22, 95% CI: 0.02 to 0.42, P (β > 0) = 0.98, respectively), whereas %Sand showed a negative association (β = -0.23, 95% CI: -0.42 to -0.03, P (β > 0) = 0.01). A positive interaction between %Sand and OM content was also detected (β = 0.19, 95% CI: 0.02 to 0.35, P (β > 0) = 0.99). Phenolic compound utilization responded positively to OM content (β = 0.21, 95% CI: 0.02 to 0.39, P (β > 0) = 0.99) and negatively to $\delta^{13}C$ values (β = -0.30, 95% CI: -0.51 to -0.08, P (β > 0) < 0.01).

In contrast, polymer utilization was negatively associated with OM content (β = -0.31, 95% CI: -0.48 to -0.14, P (β > 0) < 0.01) and positively associated with $\delta^{13}C$ values (β = 0.28, 95% CI: 0.08 to 0.48, P (β > 0) = 1.00). A positive interaction between %Fine and OM content was also detected (β = 0.23, 95% CI: 0.05 to 0.41, P (β > 0) > 0.99), indicating that the negative effect of OM on polymer utilization became progressively weaker with increasing fine material content.

Overall, vegetation-related variables showed little support across models. Neither vegetation greenness metric (NDVI) was retained in the final model set, and distance to the nearest *Z. lotus* individual showed no consistent effects on either general microbial functional metrics or C-source utilization patterns.

https://doi.org/10.5194/egusphere-2026-4227
Preprint. Discussion started: 19 August 2026

445

Table 2. Summary of the most parsimonious Bayesian models explaining variation in four general microbial functional metrics: average well colour development (AWCD), Shannon diversity (H′), Shannon evenness (E), and carbon-source richness (SR). RDTGW, relative depth to the groundwater table; OM, organic matter content of geological substrate (%); $\delta^{13}C$, stable carbon isotope composition of geological substrate; fine fraction of geological substrate (%); %Sand, sand
450 fraction of geological substrate (%); PCA1 and PCA2, scores of the first and second principal component axes, respectively, derived from groundwater physicochemical variables; Min_Dist_Z, minimum distance (m) from each borehole to the nearest *Ziziphus lotus* individual. Bold values indicate parameter estimates with strong posterior support, defined as 95% credible intervals that do not overlap zero.

C-source		Amines	Amino Acids	Carbohydrates	Carboxylic Acids	Phenolic Compounds	Polymers
Best model		RDTGW + OM + δ13C + %Fine + %Sand + PCA1 + PCA2 + Min_Dist_Z	RDTGW x OM + δ13C + %Fine + %Sand + PCA1 + PCA2 + Min_Dist_Z	δ13C x OM + RDTGW + %Fine + %Sand + PCA1+ PCA2 + Min_Dist_Z	%Sand x OM + RDTGW + δ13C + %Fine + PCA1+ PCA2 + Min_Dist_Z	RDTGW x OM + δ13C + %Fine + %Sand + PCA1 + PCA2 + Min_Dist_Z	%Fine x OM + RDTGW + δ13C + %Sand + PCA1+ PCA2 + Min_Dist_Z
SD (Bore random effect)		0.16	0.21	0.53	0.28	0.38	0.55
Sigma		0.93	1.03	0.92	0.91	0.95	0.88
Total R^2		0.17	0.12	0.23	0.25	0.22	0.29
(95% CI)		(0.09, 0.26)	(0.05, 0.20)	(0.13, 0.33)	(0.15, 0.34)	(0.12, 0.32)	(0.18, 0.39)
Intercept	Mean	-0.06	-0.01	0.03	-0.06	0.03	-0.12
	95% CI	-0.28, 0.16	-0.27, 0.24	-0.39, 0.44	-0.35, 0.24	-0.31, 0.37	-0.55, 0.31
	P (β > 0)	0.25	0.44	0.55	0.31	0.57	0.25
RDTGW	Mean	0.18	0.03	0.13	-0.08	0.21	0.06
	95% CI	-0.01, 0.37	-0.23, 0.30	-0.09, 0.35	-0.29, 0.12	-0.04, 0.46	-0.14, 0.27
	P (β > 0)	0.97	0.59	0.88	0.22	0.95	0.73
OM	Mean	-0.04	-0.04	**0.20**	**0.41**	**0.21**	**-0.31**
	95% CI	-0.22, 0.13	-0.24, 0.15	**0.02, 0.38**	**0.22, 0.60**	**0.02, 0.39**	**-0.48, -0.14**
	P(β>0)	0.30	0.33	**0.99**	**> 0.99**	**0.99**	**< 0.01**
δ13C	Mean	-0.15	-0.13	-0.11	**0.22**	**-0.30**	**0.28**
	95% CI	-0.35, 0.05	-0.35, 0.09	-0.31, 0.11	**0.02, 0.42**	**-0.51, -0.08**	**0.08, 0.48**
	P(β>0)	0.07	0.12	0.16	**0.98**	**< 0.01**	**> 0.99**
%Fine	Mean	0.07	0.15	0.01	-0.20	0.15	-0.14
	95% CI	-0.11, 0.26	-0.06, 0.35	-0.18, 0.20	-0.41, 0.01	-0.05, 0.35	-0.33, 0.05
	P(β>0)	0.77	0.92	0.55	0.03	0.92	0.07
%Sand	Mean	-0.13	-0.07	**-0.18**	**-0.23**	-0.12	0.17
	95% CI	-0.30, 0.03	-0.25, 0.13	**-0.36, 0.00**	**-0.42, -0.03**	-0.31, 0.06	-0.02, 0.36
	P(β>0)	0.06	0.24	**0.03**	**0.01**	0.08	0.96
PCA1	Mean	0.03	-0.01	-0.06	0.14	0.14	-0.13
	95% CI	-0.20, 0.24	-0.27, 0.26	-0.46, 0.33	-0.15, 0.42	-0.20, 0.45	-0.55, 0.30
	P(β>0)	0.62	0.48	0.36	0.86	0.83	0.24
PCA2	Mean	-0.08	0.02	-0.06	0.20	-0.09	-0.04
	95% CI	-0.39, 0.25	-0.34, 0.38	-0.54, 0.42	-0.21, 0.56	-0.51, 0.35	-0.53, 0.46
	P(β>0)	0.31	0.54	0.40	0.87	0.31	0.42
Min_Dist_Z	Mean	-0.18	-0.04	-0.06	0.31	0.01	-0.02
	95% CI	-0.50, 0.16	-0.42, 0.36	-0.56, 0.50	-0.14, 0.68	-0.43, 0.49	-0.55, 0.52
	P(β>0)	0.13	0.41	0.40	0.93	0.51	0.47
RDTGW x OM	Mean	--	0.21	--	--	0.16	--
	95% CI	--	-0.01, 0.43	--	--	-0.05, 0.36	--
	P(β>0)	--	0.97	--	--	0.93	--
δ13C x	Mean	--	--	**-0.20**	--	--	--
	95% CI	--	--	**-0.37, -0.02**	--	--	--

https://doi.org/10.5194/egusphere-2026-4227
Preprint. Discussion started: 19 August 2026

OM	P(β>0)	--	--	**0.01**	--	--	--
%Sand	Mean	--	--	--	**0.19**	--	--
x	95% CI	--	--	--	**0.02, 0.35**	--	--
OM	P(β>0)	--	--	--	**0.99**	--	--
%Fine	Mean	--	--	--	--	--	**0.23**
x	95% CI	--	--	--	--	--	**0.05, 0.41**
OM	P(β>0)	--	--	--	--	--	**0.99**

4 Discussion

Understanding how microbial functioning is organized across saturated-unsaturated transitions remains a central challenge in CZ research, particularly in arid environments where resource distributions are highly heterogeneous and hydrological connectivity is spatially and temporally variable. Our results indicate that microbial functional responses were only weakly associated with the broad hydrological organization of the profile and were instead linked to multiple hydrobiogeochemical controls operating across the CZ continuum.

4.1 Hydrobiogeochemical heterogeneity across the CZ continuum

The central finding of this study is that microbial functional organization across the arid CZ we examined does not follow the depth-dependent, zonation-based structure predicted by conventional CZ conceptual models. Saturated-unsaturated partitioning per se - a key organizing boundary in humid-climate CZ frameworks - emerged as a weak predictor of the microbial functional profiles assessed here. Instead, microbial functional responses were more strongly associated with microscale heterogeneity in resource availability and substrate conditions than with position along the vertical profile, supporting our first hypothesis and indicating that variation in OM availability, substrate texture, and OM processing exerted a stronger influence on microbial functional profiles than broad hydrological partitioning (Brantley et al., 2007; Chorover et al., 2007; Akob and Küsel, 2011; Wu et al., 2023). The weak influence of relative depth to the groundwater table further supports this interpretation, suggesting that vertical position was not a primary driver of the functional responses observed (Fierer et al., 2003; Or et al., 2007; Allison and Martiny, 2008). Under the resource-limited conditions characteristic of arid ecosystems, OM availability and substrate texture may exert particularly strong influences on microbial functioning (Schimel et al., 2007; Bastida et al., 2021). In contrast to conceptual models developed for more humid CZs, where subsurface organization is often associated with relatively continuous vertical gradients in hydrology, weathering, and biogeochemical development (Brantley et al., 2007; Chorover et al., 2007; Rempe and Dietrich, 2018), microbial functioning in arid CZs may be more strongly shaped by localized hydrobiogeochemical mosaics and spatially discontinuous resource distributions, partially decoupling microbial functional organization from the broad hydrological gradients that underpin many existing CZ frameworks (Or et al., 2007; Allison and Martiny, 2008; Bastida et al., 2021).

https://doi.org/10.5194/egusphere-2026-4227
Preprint. Discussion started: 19 August 2026

4.2 Organic matter controls

OM availability emerged as the dominant control on microbial functioning across the CZ profile, supporting our second hypothesis, whereas OM quality exerted more selective effects on microbial metabolism and C-source utilization. The pervasive positive effects of substrate OM content on AWCD, H′, E, SR, and the utilization of several C-source groups indicate that organic resource availability regulates microbial functioning within this arid subsurface environment (Schimel et al., 2007; Bastida et al., 2016). In water-limited ecosystems, microbial activity tends to concentrate around localized C-rich microsites and resource hotspots (Schimel et al., 2007; Kuzyakov and Blagodatskaya, 2015; Bastida et al., 2021), consistent with the broad influence of OM on multiple microbial functional metrics observed in this study. In contrast to these general positive effects of OM on microbial functioning, potential polymer utilization declined with increasing OM content. Under OM-rich conditions, microbial communities may rely proportionally more on relatively labile C sources, thereby reducing the relative contribution of polymers to total C-source utilization (Cotrufo et al., 2013; Kuzyakov and Blagodatskaya, 2015; Lehmann and Kleber, 2015).

While OM quantity exerted broad effects across most microbial functional metrics, $\delta^{13}C$-related patterns suggest that OM quality influenced how microbial communities allocated resource-use strategies among different C-source groups. The negative effect of $\delta^{13}C$ on AWCD suggests that OM processing primarily affected microbial metabolic intensity rather than the overall organization of C-source utilization. Increasing $\delta^{13}C$ values may reflect lower energetic quality and a greater degree of OM processing (Ehleringer et al., 2000; Lehmann and Kleber, 2015; Krüger et al., 2024). Such isotopic enrichment is commonly interpreted as a signature of progressive OM processing, resulting from the combined effects of selective retention of ^{13}C-depleted compounds and preferential microbial mineralization of ^{12}C-enriched organic matter during downward transport through the CZ (Kaiser et al., 2001; Wynn et al., 2006; Boström et al., 2007). These processes could constrain total microbial activity without substantially altering the diversity, evenness, or range of C-sources utilized by microbial communities (Fierer et al., 2003; Allison and Martiny, 2008; Bowling et al., 2008). $\delta^{13}C$ also exerted selective effects on particular metabolic pathways, as reflected by the contrasting responses observed among C-source groups. The negative association between $\delta^{13}C$ and phenolic compound utilization suggests that increasingly processed OM conditions may reduce the relative importance of phenolic C sources for microbial metabolism (Ehleringer et al., 2000; Bowling et al., 2008). In contrast, the positive associations observed for carboxylic acid and polymer utilization indicate a shift in microbial resource-use patterns under these conditions, favouring relatively oxidized compounds as well as structurally complex C sources (Cotrufo et al., 2013; Lehmann and Kleber, 2015). The recurrent negative interactions between $\delta^{13}C$ and OM across several models further support this interpretation, indicating that the positive effects of OM availability weakened under conditions associated with increasingly processed OM.

Taken together, the OM-related findings reinforce the broader interpretation that microbial functioning in this arid CZ is organized primarily around localized resource availability rather than around vertical biogeochemical gradients. In humid CZs, vertical gradients in OM quantity and quality are often tightly coupled to depth and hydrological position, producing

https://doi.org/10.5194/egusphere-2026-4227
Preprint. Discussion started: 19 August 2026

relatively predictable depth profiles of microbial activity (Fierer et al., 2003; Lehmann and Kleber, 2015). In the present system, OM availability exhibited substantial spatial variability with only weak vertical organization, whereas OM quality showed a clearer depth-related pattern and significant differences between saturated and unsaturated zones. However, this vertical structuring of OM quality did not translate into a corresponding depth-dependent organization of microbial functional profiles. Instead, multiple CLPP-derived functional metrics responded more strongly to local OM availability and quality than to position along the profile itself. These results suggest that resource patchiness and localized hydrobiogeochemical heterogeneity, rather than vertical zonation, constitute the primary organizing forces of microbial functioning in this arid CZ. More broadly, they indicate that the existence of vertical geochemical gradients alone is insufficient to generate the vertically organized biogeochemical and microbial patterns commonly described for humid-climate CZs (Brantley et al., 2007; Chorover et al., 2007; Rempe and Dietrich, 2018).

4.3 Texture-mediated responses

Although substrate texture exhibited relatively limited variation across the CZ profile, it emerged as a consistent predictor of microbial functioning in the models. These results suggest that substrate texture can exert disproportionate effects on microbial functioning by regulating pore-scale environmental conditions and habitat heterogeneity (Young and Crawford, 2004; Or et al., 2007; Nunan et al., 2020). In porous subsurface environments, texture regulates water retention, oxygen diffusion, pore connectivity, and the spatial distribution and physical protection of organic resources, thereby shaping microbial activity and microsite resource heterogeneity (Six et al., 2002; Young and Crawford, 2004; Or et al., 2007). The recurrent negative effects associated with sandy fractions across multiple CLPP-derived metrics and several C-source utilization groups likely reflect the lower moisture retention and reduced capacity for OM stabilization typically associated with coarse-textured substrates (Or et al., 2007; Schimel et al., 2007; Six et al., 2002; Cotrufo et al., 2013; Cyle et al., 2016). The positive %Sand × OM interactions observed for several microbial functional metrics suggest that OM availability partially compensated for the constraints associated with sandy substrates, consistent with the idea that localized resource accumulation may generate microbial hotspots even under physically limiting conditions (Young and Crawford, 2004; Kuzyakov and Blagodatskaya, 2015; Nunan et al., 2020). By comparison, fine material content exhibited only weak positive effects on AWCD and E, likely because enhanced moisture retention and organo-mineral stabilization may locally promote microbial activity and a more even use of C sources (Six et al., 2002; Or et al., 2007; Cotrufo et al., 2013). However, the positive %Fine × OM interaction observed for polymer utilization suggests that fine-textured materials may also influence the fate of structurally complex organic compounds. Under OM-rich conditions, the relative decline in polymer utilization was less pronounced in substrates containing higher proportions of fine material, potentially reflecting the capacity of finer fractions to stabilize these compounds through organo-mineral associations and microscale protection mechanisms (Six et al., 2002; Lehmann and Kleber, 2015). Overall, texture acted primarily as a modifier of OM effects rather than as a primary control on microbial functioning (Schimel et al., 2007; Kuzyakov and Blagodatskaya, 2015; Bastida et al., 2021).

https://doi.org/10.5194/egusphere-2026-4227
Preprint. Discussion started: 19 August 2026

4.4 Limited vegetation influences

Contrary to our third hypothesis, vegetation-related variables exerted only limited influences on microbial functioning across the CZ profile. Neither proximity to *Z. lotus* individuals nor vegetation greenness emerged as major drivers of microbial functioning. Although deep-rooted phreatophytic vegetation can influence groundwater-associated biogeochemical and microbial processes through rhizosphere C inputs and groundwater redistribution (Griebler and Lueders, 2009; Eamus et al., 2015), these effects were not detected as dominant controls on the microbial functional responses assessed here. This may reflect the sparse and patchy distribution of vegetation in arid ecosystems, which generates spatially discontinuous rhizosphere interactions that remain largely confined to root-influenced microsites rather than extending across the broader subsurface matrix (Schlesinger et al., 1996; Okin et al., 2015). Previous work in the same ecosystem documented marked rhizosphere effects associated with *Z. lotus* in surface soils (Torres-García et al., 2022). However, a physiological threshold around 14 m groundwater depth, beyond which *Z. lotus* individuals experience increasing water stress (Torres-García et al., 2021b), likely limits belowground C allocation at depth and further constrains rhizosphere stimulation across the CZ (Naumburg et al., 2005; Eamus et al., 2006). Importantly, the absence of detectable *Z. lotus* effects on subsurface microbial functioning is, in our view, not merely a null result but a substantively informative one. *Z. lotus* is a structurally dominant species with roots documented at depths up to 60 m (Le Houérou, 2006), substantial groundwater uptake, and soil-level biogeochemical effects (Torres-García et al., 2021b; Torres-García et al., 2022). The fact that a species with such extensive rooting systems and documented biogeochemical effects does not produce a detectable footprint in subsurface microbial functioning underscores how strongly spatial discontinuity governs resource distribution in arid CZs. If even a species of this ecological stature cannot homogenize microbial functioning across the subsurface profile, it is difficult to attribute the spatial patterns we observe to any vegetation-mediated process operating at profile scale. This reinforces the interpretation that the relevant organizational unit in arid CZs is not the vertical profile or the plant neighbourhood, but the microsite - the localized patch of resource availability that determines microbial functioning independently of its position in the broader landscape context.

Collectively, these results reinforce the view that arid CZs are organized by principles that diverge from the humid-climate template on which most CZ conceptual models were originally developed. The vertical-gradient framework remains highly effective for the systems in which it was established, but the present findings suggest that complementary conceptual models are needed for drylands, where spatial discontinuity, episodic hydrology, and microscale resource heterogeneity may act as primary organizing forces. The present study provides empirical support for such models and highlights the saturated-unsaturated transition as a boundary that is biogeochemically important in humid systems but loses much of its organizing power in arid ones.

https://doi.org/10.5194/egusphere-2026-4227
Preprint. Discussion started: 19 August 2026

5 Conclusions

Conventional conceptual models of the CZ describe subsurface ecosystem organization in terms of continuous vertical gradients tied to the saturated-unsaturated transition. This study provides evidence that such a framework may not adequately describe the microbial functional profiles observed in this arid CZ, where the measured functional responses were more strongly associated with spatially localized hydrobiogeochemical heterogeneity than with depth-based or zonation-based gradients. These results suggest that arid and humid CZs may operate under substantially different organizational principles. Within this arid system, OM availability emerged as the dominant control on microbial functional responses - driving overall metabolic activity, functional diversity, evenness, and C-source richness - while OM processing and substrate texture exerted more selective influences on specific microbial responses and C-source utilization patterns. Relative depth to the groundwater table, proximity to *Z. lotus* individuals, and vegetation greenness showed comparatively weak effects. The absence of detectable vegetation effects is particularly informative: the failure of a structurally dominant deep-rooted phreatophyte to organize microbial functioning at profile scale supports the interpretation that spatial discontinuity, rather than vertical position or plant neighbourhood, is the primary organizational unit of this arid CZ. These findings highlight the need to move beyond depth-based conceptualizations of subsurface ecosystem organization when working in dryland systems. As arid regions expand under climate change and CZ research increasingly extends into dryland settings, developing arid-specific conceptual models that recognize microscale resource heterogeneity and spatially discontinuous hydrobiogeochemical organization as first-order principles will be essential for understanding and predicting subsurface ecosystem functioning under water limitation.

Code and data availability

The dataset used in this study are available from Zenodo at https://doi.org/10.5281/zenodo.21247246 (Salinas-Bonillo and Cabello, 2026).

Supplement link

The link to the supplement will be included by Copernicus, if applicable.

Author contributions

JC, MJL, and MJSB: Conceptualization, Supervision. CG, AFC, and MRMG: Laboratory analyses. LCA, MEC, JG and MJSB: Formal analysis. MJSB: Data curation, Writing – original draft. JC: Funding acquisition. All authors: Writing – review & editing, and approval of the final manuscript.

https://doi.org/10.5194/egusphere-2026-4227
Preprint. Discussion started: 19 August 2026

Competing interests

The contact author has declared that none of the authors has any competing interests.

Disclaimer

Copernicus Publications remains neutral with regard to jurisdictional claims made in the text, published maps, institutional affiliations, or any other geographical representation in this paper. The authors bear the ultimate responsibility for providing appropriate place names. Views expressed in the text are those of the authors and do not necessarily reflect the views of the publisher.

Acknowledgements

The authors gratefully acknowledge the Andalusian Centre for Global Change (ENGLOBA), the Stable Isotope Laboratory, and the research groups RNM174 - Ecozonar (Ecology of Arid Zones), RNM189 - Water Resources and Environmental Geology, and BIO175 - Technological Development of Microbiological Approaches for the Improvement of Agricultural Soils, all at the University of Almería, for providing access to their laboratory facilities and technical infrastructure, which made this research possible.

Financial support

This research was conducted within the framework of the LTSER Platform “The Arid Iberian South East LTSER Platform-Spain” (LTER_EU_ES_027) and was supported by the European Union through the projects LIFE ADAPTAMED (LIFE14 CCA/ES/000612), LIFEWATCH-INDALO (LIFEWATCH-2019-04-AMA-01), and “Indicators for Monitoring the Supply and Demand of Ecosystem Functions and Services” (SP4-LiA3).

Review statement

The review statement will be added by Copernicus Publications listing the handling editor as well as all contributing referees according to their status anonymous or identified.

References

Akob, D. M., and Küsel, K.: Where microorganisms meet rocks in the Earth’s Critical Zone, Biogeosciences, 8, 3531–3543, https://doi.org/10.5194/bg-8-3531-2011, 2011.

https://doi.org/10.5194/egusphere-2026-4227
Preprint. Discussion started: 19 August 2026

Allison, S. D., and Martiny, J. B. H.: Resistance, resilience, and redundancy in microbial communities, PNAS, 105(1); 11512–11519, https://doi.org/10.1073/pnas.0801925105, 2008.

Bastida, F., Eldridge, D. J., García, C., Kenny Png, G., Bardgett, R. D., and Delgado-Baquerizo, M.: Soil microbial diversity-biomass relationships are driven by soil carbon content across global biomes, ISME J., 15(7), 2081–2091, https://doi.org/10.1038/s41396-021-00906-0, 2021.

Bastida, F., Torres, I. F., Moreno, J. L., Baldrian, P., Ondoño, S., Ruiz-Navarro, A., Hernández, T., Richnow, H.-H., Starke, R., García, C., and Jehmlich, N.: The active microbial diversity drives ecosystem multifunctionality and is physiologically related to carbon availability in Mediterranean semi-arid soils, Mol. Ecol., 25(18), 4660–4673, https://doi.org/10.1111/mec.13783, 2016.

Boström, B., Comstedt, D. and Ekblad, A.: Isotope fractionation and 13C enrichment in soil profiles during the decomposition of soil organic matter, Oecologia, 153, 89–98, https://doi.org/10.1007/s00442-007-0700-8, 2007.

Bowling, D. R., Pataki, D. E., and Randerson, J. T.: Carbon isotopes in terrestrial ecosystem pools and CO_2 fluxes, New Phytol., 178(1), 24–40, https://doi.org/10.1111/j.1469-8137.2007.02342.x, 2008.

Brantley, S. L., Goldhaber, M. B., and Ragnarsdottir, K.V.: Crossing disciplines and scales to understand the critical zone, Elements 3(5), 307–314, https://doi.org/10.2113/gselements.3.5.307, 2007.

Chorover, J., Kretzschmar, R., Garcia-Pichel, F., and Sparks, D. L.: Soil biogeochemical processes within the critical zone, Elements, 3(5), 321–326, https://doi.org/10.2113/gselements.3.5.321, 2007.

Cotrufo, M. F., Wallenstein, M. D., Boot, C. M., Denef, K., and Paul, E.: The Microbial Efficiency-Matrix Stabilization (MEMS) framework integrates plant litter decomposition with soil organic matter stabilization: do labile plant inputs form stable soil organic matter?, Glob. Change Biol., 19, 988–995. https://doi.org/10.1111/gcb.12113, 2013.

Cyle, K. T., Hill, N., Young, K., Jenkins, T., Hancock, D., Schroeder, P. A., and Thompson, A.: Substrate quality influences organic matter accumulation in the soil silt and clay fraction, Soil Biol. Biochem., 103, 138–148, https://doi.org/10.1016/j.soilbio.2016.08.014, 2016.

Das, B. M., and Sobhan, K.: Principles of Geotechnical Engineering, Cengage Learning, Boston, MA, USA, 819 pp., ISBN 9781305970939, 2018.

Eamus, D., Froend, R., Loomes, R., Hose, G., and Murray, B.: A functional methodology for determining the groundwater regime needed to maintain the health of groundwater-dependent vegetation, Aust. J. Bot., 54(2), 97–114, https://doi.org/10.1071/BT05031, 2006.

Eamus, D., Zolfaghar, S., Villalobos-Vega, R., Cleverly, J., and Huete, A.: Groundwater-dependent ecosystems: recent insights from satellite and field-based studies, Hydrol. Earth Syst. Sci., 19, 4229–4256, https://doi.org/10.5194/hess-19-4229-2015, 2015.

Ehleringer, J. R., Roden, J., and Dawson, T. E.: Assessing ecosystem-level water relations through stable isotope ratio analyses, in: Methods in Ecosystem Science, edited by: Sala, O. E., Jackson, R. B., Mooney, H. A., and Howarth R. W., Springer, New York, NY, USA, 181–198. https://doi.org/10.1007/978-1-4612-1224-9_13, 2000.

https://doi.org/10.5194/egusphere-2026-4227
Preprint. Discussion started: 19 August 2026

Feigl, V., Ujaczki, E., Vaszita, E., and Molnár, M.: Influence of red mud on soil microbial communities: Application and comprehensive evaluation of the Biolog EcoPlate approach as a tool in soil microbiological studies, Sci. Total Environ., 595, 903–911, https://doi.org/10.1016/j.scitotenv.2017.03.266, 2017.

Fierer, N., Schimel, J. P., and Holden, P. A.: Variations in microbial community composition through two soil depth profiles, Soil Biol. Biochem., 35(1), 167–176, https://doi.org/10.1016/S0038-0717(02)00251-1, 2003.

Garland, J. L.: Patterns of potential C source utilization by rhizosphere communities, Soil Biol. Biochem., 28(2), 223–230, https://doi.org/10.1016/0038-0717(95)00113-1, 1996.

Griebler, C., and Lueders, T.: Microbial biodiversity in groundwater ecosystems, Freshw. Biol., 54(4), 649–677, https://doi.org/10.1111/j.1365-2427.2008.02013.x, 2009.

Guirado, E., Alcaraz-Segura, D., Rigol-Sánchez, J. P., Gisbert, J., Martínez-Moreno, F. J., Galindo-Zaldívar, J., González-Castillo, L., and Cabello, J.: Remote-sensing-derived fractures and shrub patterns to identify groundwater dependence, Ecohydrology, 11, e1933, https://doi.org/10.1002/eco.1933, 2018.

Guirado, E., Blanco-Sacristán, J., Rigol-Sánchez, J. P., Alcaraz-Segura, D., and Cabello, J.: A multi-temporal object-based image analysis to detect long-lived shrub cover changes in drylands, Remote Sens., 11(22), 2649, https://doi.org/10.3390/rs11222649, 2019.

Kaiser, K., Guggenberger, G., and Zech, W.: Isotopic fractionation of dissolved organic carbon in shallow forest soils as affected by sorption, Eur. J. Soil Sci., 52(4): 585–597, https://doi.org/10.1046/j.1365-2389.2001.00407.x, 2001.

Krüger, N., Finn, D. R., and Don, A.: Soil depth gradients of organic carbon-13 - A review on drivers and processes, Plant Soil, 495, 113–136, https://doi.org/10.1007/s11104-023-06328-5, 2024.

Kuzyakov, Y., and Blagodatskaya, E.: Microbial hotspots and hot moments in soil: Concept & review, Soil Biol. Biochem., 83, 184–199, https://doi.org/10.1016/j.soilbio.2015.01.025, 2015.

Le Houérou, H. N.: Agroforestry and silvopastoralism: the role of trees and shrubs (trubs) in range rehabilitation and development, Sécheresse, 17, 343–348, 2006.

Legendre, P., and Gallagher, E. D.: Ecologically meaningful transformations for ordination of species data, Oecologia, 129, 271–280, https://doi.org/10.1007/s004420100716, 2001.

Lehmann, J., and Kleber, M.: The contentious nature of soil organic matter, Nature, 528, 60–68, https://doi.org/10.1038/nature16069, 2015.

Machado, M. J., Benito, G., Barriendos, M., and Rodrigo, F. S.: 500 Years of rainfall variability and extreme hydrological events in southeastern Spain drylands, J. Arid Environ., 75(12), 1244–1253, https://doi.org/10.1016/j.jaridenv.2011.02.002, 2011.

National Research Council (Ed.): Basic Research Opportunities in Earth Science, National Academy Press, Washington, DC, USA, https://doi.org/10.17226/9981, 154 pp. ISBN 0309569885, 2001.

https://doi.org/10.5194/egusphere-2026-4227
Preprint. Discussion started: 19 August 2026

Naumburg, E., Mata-Gonzalez, R., Hunter, R. G., McLendon, T., and Martin, D. W.: Phreatophytic vegetation and groundwater fluctuations: a review of current research and application of ecosystem response modeling with an emphasis on Great Basin vegetation, Environ. Manag., 35, 726–740, https://doi.org/10.1007/s00267-004-0194-7, 2005.

Németh, I., Molnár, S., Vaszita, E., and Molnár, M.: The Biolog EcoPlate™ technique for assessing the effect of metal oxide nanoparticles on freshwater microbial communities, Nanomaterials, 11(7), 1777, https://doi.org/10.3390/nano11071777, 2021.

Nunan, N., Schmidt, H., and Raynaud, X.: The ecology of heterogeneity: soil bacterial communities and C dynamics, Philos. Trans. R. Soc. Lond. B Biol. Sci., 375, 20190249, https://doi.org/10.1098/rstb.2019.0249, 2020.

Okin, G. S., Moreno-de las Heras, M., Saco, P. M., Throop, H. L., Vivoni, E. R., Parsons, A. J., Wainwright, J. and Peters, D. P.: Connectivity in dryland landscapes: shifting concepts of spatial interactions, Front. Ecol. Environ., 13(1), 20–27, https://doi.org/10.1890/140163, 2015.

Or, D., Smets, B. F., Wraith, J. M., Dechesne, A., and Friedman, S. P.: Physical constraints affecting bacterial habitats and activity in unsaturated porous media – a review, Adv. Water Resour., 30(6-7), 1505–1527, https://doi.org/10.1016/j.advwatres.2006.05.025, 2007.

Paruelo, J. M., Epstein, H. E., Lauenroth, W. K., and Burke, I. C.: ANPP estimates from NDVI for the central grassland region of the United States, Ecology, 78, 953–958, https://doi.org/10.2307/2266073, 1997.

Philippot, L., Raaijmakers, J., Lemanceau, P., and van der Putten, W. H.: Going back to the roots: the microbial ecology of the rhizosphere, Nat. Rev. Microbiol., 11, 789–799. https://doi.org/10.1038/nrmicro3109, 2013.

Preston-Mafham, J., Boddy, L., and Randerson, P. F.: Analysis of microbial community functional diversity using sole-carbon-source utilisation profiles – a critique, FEMS Microbiol. Ecol., 42(1), 1–14, https://doi.org/10.1111/j.1574-6941.2002.tb00990.x, 2002.

Rempe, D. M., and Dietrich, W. E.: Direct observations of rock moisture, a hidden component of the hydrologic cycle, PNAS, 115(11), 2664–2669, https://doi.org/10.1073/pnas.1800141115, 2018.

Rouse, J. W., Hass, R. H., Schell, J. A., and Deering, D. W.: Monitoring vegetation systems in the Great Plains with ERTS, Proceedings of the Goddard Space Flight Center 3d ERTS-1 Symposium, 1, pp. 309–317, https://ntrs.nasa.gov/citations/19740022614, 1974.

Schlesinger, W. H., Raikes, J. A., Hartley, A. E., and Cross, A. F.: On the spatial pattern of soil nutrients in desert ecosystems, Ecology 77(2), 364–374, https://doi.org/10.2307/2265615, 1996.

Schimel, J., Balser, T. C., and Wallenstein, M.: Microbial stress-response physiology and its implications for ecosystem function, Ecology, 88(6), 1386–1394, https://doi.org/10.1890/06-0219, 2007.

Schwinning, S., and Sala, O. E.: Hierarchy of responses to resource pulses in arid and semi-arid ecosystems, Oecologia, 141, 211–220, https://doi.org/10.1007/s00442-004-1520-8, 2004.

Six, J., Conant, R. T., Paul, E. A., and Paustian, K.: Stabilization mechanisms of soil organic matter: Implications for C-saturation of soils, Plant Soil, 241, 155–176, https://doi.org/10.1023/A:1016125726789, 2002.

https://doi.org/10.5194/egusphere-2026-4227
Preprint. Discussion started: 19 August 2026

Soldatova, E., Krasilnikov, S., and Kuzyakov, Y.: Soil organic matter turnover: Global implications from δ13C and δ15N signatures, Sci. Total Environ., 912, 169423, https://doi.org/10.1016/j.scitotenv.2023.169423, 2024.

Sparkes, R. B., Rae, S. A., McMahon, L., Mossman, H. L., McKendry, D., Dean, C. E., Tinsley, G., Fowden, F., Grisdale, C. J., Begum, H., Hope, H., McEnhill, C., O'Boyle, S., Sohail, N., Wachira, M., and Dunk, R. M.: Comparing loss-on-ignition, acid decarbonation and combustion elemental analysis for measuring organic carbon concentrations - recommendations for best practice, Org. Geochem., 218, 105215, https://doi.org/10.1016/j.orggeochem.2026.105215, 2026.

Tian, F., Brandt, M., Liu, Y. Y., Rasmussen, K., and Fensholt, R.: Mapping gains and losses in woody vegetation across global tropical drylands, Glob. Chang. Biol., 23(4), 1748–1760. https://doi.org/10.1111/gcb.13464, 2017.

Tirado, R.: 5220 Matorrales arborescentes con *Ziziphus* (*), in: Bases ecológicas preliminares para la conservación de los tipos de hábitat de interés comunitario en España, edited by VV.AA., Ministerio de Medio Ambiente, y Medio Rural y Marino, Madrid, Spain, 1–68, 2009.

Torres-García, T., Salinas-Bonillo, M. J., Cleverly, J. R., Gisbert, J., Pacheco-Romero, M., and Cabello, J.: A multiple-trait analysis of ecohydrological acclimatisation in a dryland phreatophytic shrub, Oecologia, 196, 1179–1193, https://doi.org/10.1007/s00442-021-04993-w, 2021a.

Torres-García, M. T., Salinas-Bonillo, M. J., Gázquez-Sánchez, F., Fernández-Cortés, A., Querejeta, J. I., and Cabello, J.: Squandering water in drylands: the water use strategy of the phreatophyte *Ziziphus lotus* in a groundwater dependent ecosystem, Am. J. Bot., 108(2), 236–248, https://doi.org/10.1002/ajb2.1606, 2021b.

Torres-García, M. T., Oyonarte, C., Cabello, J., Guirado, E., Rodríguez-Lozano, B., and Salinas-Bonillo, M. J.: The potential of groundwater-dependent ecosystems to enhance soil biological activity and soil fertility in drylands, Sci. Total Environ., 826, 154111, https://doi.org/10.1016/j.scitotenv.2022.154111, 2022.

Vallejos, A., Sola, F., Yechieli, Y., and Pulido-Bosch, A.: Influence of the paleogeographic evolution on the groundwater salinity in a coastal aquifer. Cabo de Gata aquifer, SE Spain, J. Hydrol., 557, 55–66, https://doi.org/10.1016/j.jhydrol.2017.12.027, 2018.

Young, I. M., and Crawford, J. W.: Interactions and self-organization in the soil-microbe complex, Science, 304(5677), 1634–1637. https://doi.org/10.1126/science.1097394, 2004.

Wang, Q., Li, Y., and Wang, Y.: Optimizing the weight loss-on-ignition methodology to quantify organic and carbonate carbon of sediments from diverse sources, Environ. Monit. Assess., 174, 241–257, https://doi.org/10.1007/s10661-010-1454-z, 2011.

Wu, X., Gushgari-Doyle, S., Lui, L.M., Hendrickson, A. J., Liu, Y., Jagadamma, S., Nielsen, T. N., Justice, N. B., Simmons, T., Hess, N. J., Joyner, D. C., Hazen, T. C., Arkin, A. P., and Chakraborty, R.: Distinct depth-discrete profiles of microbial communities and geochemical insights in the subsurface critical zone, Appl. Environ. Microbiol., 89(6), e00500-23, https://doi.org/10.1128/aem.00500-23, 2023.

https://doi.org/10.5194/egusphere-2026-4227
Preprint. Discussion started: 19 August 2026

Wynn, J. G., Harden, J. W., and Fries, T. L.: Stable carbon isotope depth profiles and soil organic carbon dynamics in the lower Mississippi Basin, Geoderma, 131(1–2), 89–109, https://doi.org/10.1016/j.geoderma.2005.03.005, 2006.

Zhang, Z., and Furman, A.: Soil redox dynamics under dynamic hydrologic regimes - A review, Sci. Total Environ., 763, 143026, https://doi.org/10.1016/j.scitotenv.2020.143026, 2021.